Spectroscopic and Electrochemical Studies on Block-Polymer/PMMA Blend based Composite Polymer Electrolytes

Shupeng Zhang,[1,2] Xiangkai Fu,[2] Yongfeng Gong[2]

[1]*College of Chemistry, Sichuan University, Chengdu 610065, People's Republic of China*
[2]*College of Chemistry and Chemical Engineering, Southwest-China University, Chongqing 400715, People's Republic of China*

Received 27 November 2006; accepted 15 May 2007
DOI 10.1002/app.26903
Published online 5 September 2007 in Wiley InterScience (www.interscience.wiley.com).

ABSTRACT: Poly(methylmethacrylate)(PMMA)/oxymethylene-linked polyoxyethylene multi-block polymer(Om-POE$_n$, where n represents number of unit $-CH_2CH_2O-$) blend based composite electrolyte films containing different lithium salt concentration and nanofillers' content are prepared using solvent evaporation technique. The interaction of polymer–salt complex has been confirmed using FTIR spectral studies. The figuration of CPE was studied by XRD. Ionic conductivity and thermal behavior of the CPEs were studied with various salt concentrations, temperature, and nanofillers' content. The surface structure of the CPE is also investigated using scanning electron microscopy. The high room temperature ionic conductivity, transmittivity in the visible region, and thermal stability make these CPEs potential candidates as solid-like electrolytes for electrochemical devices. © 2007 Wiley Periodicals, Inc. J Appl Polym Sci 106: 4091–4097, 2007

Key words: blends; polyelectrolytes; FTIR; thermogravimetric analysis (TGA); X-ray

INTRODUCTION

Polymer electrolytes are attracting increasing attention because of promising applications such as solid-state rechargeable lithium-ion batteries, supercapacitors, and electrochromic devices (ECD).[1] The main advantage of polymer electrolytes are relatively high ionic conductivity, favorable mechanical properties, ease of fabrication of thin films of desirable size, and an ability to form effective electrode–electrolyte contacts.

Numerous conventional and technological studies on electrolytes including different polymer matrix such as PEO, PMMA, PVdF, PAN, etc. have been reported.[2–8] Because of the high crystallinity, the high room temperature ionic conductivities have not yet been achieved unfortunately.

To enhance the high room temperature ionic conductivity, various approaches such as using blends,[9,10] copolymers,[11] comb-branch polymers,[12] crosslinked networks,[13] and adding plasticizers[14] have been developed. All improvements have been achieved either by reducing the crystallinity of the polymers or by lowering the glass transition temperature. It is generally observed, however, that high conductivity is achieved at the expense of good dimensional stability.[15]

Correspondence to: X. Fu (fxk@swu.edu.cn).

Journal of Applied Polymer Science, Vol. 106, 4091–4097 (2007)

To improve the electrochemical and mechanical properties of polymer electrolytes, composite polymer electrolytes formed by adding inorganic fillers to the gel polymer electrolytes are proposed by Weston and Steele.[16] And, many important efforts have been achieved.[17–19] The conductivity enhancement is commonly attributed to a decrease in polymer crystallinity, and an enlargement of the amorphous domain in the polymer matrix.

The ECD have acquired keen interests because of lots of potential applications, such as smart windows, new type of electronic display material, and new communication media ''electronic paper'' display devices.[20] ECD usually consist of a structure of the following layers: ITO glass || electrochromic film of viologen derivative || electrolyte film || ion storage layers || ITO glass. Ion conducting electrolyte is an important layer in the ECD and plays transporting ions and conducting current roles between the electrochromic and the ion storage layers. So, the goal of polymer electrolyte research to satisfy for ECD in our group has been to develop polymer electrolytes with higher room temperature ionic conductivity, higher optical clarity in the visible region, good mechanical properties, and thermal stability at the same time.

Polymer electrolytes based on polymer blends are useful approach that has witted a great potential in overcoming the drawbacks of polymer electrolytes mentioned above.[21–25] The problem in choosing polymer blends is the miscibility of the components. By

careful selection of the support polymer, there may be the added advantage of lowering the degree of crystallinity.[22] Combinations of proton-donating and proton-accepting polymers can form intermacromolecular complexes in aqueous or organic media.[26,27] PMMA and Om-POE$_n$ form one such couple.

In our work, CPE membranes consisting of PMMA, Om-POE$_n$, $LiClO_4$, PC, and nanofillers are prepared and characterized by FTIR, ac impedance spectroscopy, transmittivity in the visible region, XRD, SEM, and DTA, a detailed analysis of which is presented here. What's more, in all literature we can search, transmittivity of composite polymer electrolytes in the visible region has not been studied in detail.

EXPERIMENTAL

Materials

PMMA (M_W: 200,000), polyethylene glycol (PEG) (M_W: 400; 600), KOH, and lithium perchlorate were supplied by Aldrich and used after drying at 100°C in a vacuum oven overnight. Synthesis grade propylene carbonate (Merck, Germany), acetonitrile (Aldrich USA), CH_2Cl_2, tetrahydrofuran (THF), toluene, and petroleum ether (bp 60–90°C) (Chongqing, China) were used after drying over 4 Å molecular sieves. Nanometer-size SiO_2 and TiO_2 (10 nm) (Nanjing, China) was used after drying in a vacuum oven for 72 h at 120°C.

Sample preparation

To a 25 g of KOH powder, 120 mL of CH_2Cl_2 and 25 g of PEG mixture (PEG400 : PEG600 = 2 : 3 wt %) were slowly added at room temperature. After the solution was stirred for 20 h, the crude product was filtrated under the reduced pressure to get rid of the KCl and unreacted KOH particles. At last, the homogeneous product was dried at 60°C in the reduced pressure vacuum for 24 h. Transparent Om-POE$_n$ was obtained by Williamson reaction.[28]

Preparation of GPEs (step 1)

Liquid electrolyte solutions were prepared on the basis of moles of lithium salt per liter of the solvent PC. Thus, electrolyte solutions of the different molar strengths (xM $LiClO_4$-PC; x = 0.4, 0.6, 0.8, 1.0, 1.2, 1.5, and 2.0) were synthesized. According to the Table I, which illustrates the ratio of miscibility of two components, to 15 mL of solution THF, the immobilizing 5 g of mixture of Om-POE$_n$ and PMMA, whose wt ratio is 1 : 4, 10 mL of liquid electrolyte in different concentration were added. The system was stirred with the help of magnetic bar at 60°C for about 12 h, till homogeneity was attained. The obtained GPE can also be used as a solid film, by using solvent evaporation techniques. The films were further dried for 24 h in vacuum at 60°C to remove any trace of THF.

TABLE I
Om-POE$_n$ and PMMA Blend Ratio in 15 mL of THF

Om-POE$_n$: PMMA (wt ratio)	State after mixing
4 : 1	Demixing
3 : 2	Demixing
1 : 3	Demixing
1 : 4	Homogeneity

Preparation of CPEs (step 2)

The CPE was obtained, after adding nanofillers in different weight percentage to the GPE system above on the base of step 1.

Instrumentation

FTIR spectroscopic studies were carried out using a Perkin–Elmer GX2000 FTIR spectrophotometer at room temperature in the frequency range 4000–500 cm^{-1}. The ionic conductivities were measured using a ZL5-LCR impedance analyzer over the temperature range 25 −80°C controlled by circulating water bath with a temperature controlled under an oscillation potential of 50 mV from 100 kHz to 1 Hz (Shanghai, China). The ionic conductivity was calculated using the formula: $\sigma = d/(S\,Rb)$, Hereby, σ is the ionic conductivity (S cm^{-1}), d is the thickness of membrane (cm), S is the contacted area of the membrane (cm^2), R is the resistance (Ω^{-1} cm^{-1}). XRD was recorded on a D/MAX-3C X-ray diffractometer (Beijing, China) using Cu Kα radiation with a scanning speed of 28 min^{-1}. The CPE was pressed a die into pellets (0.25 mm thick) sandwiched between two slices

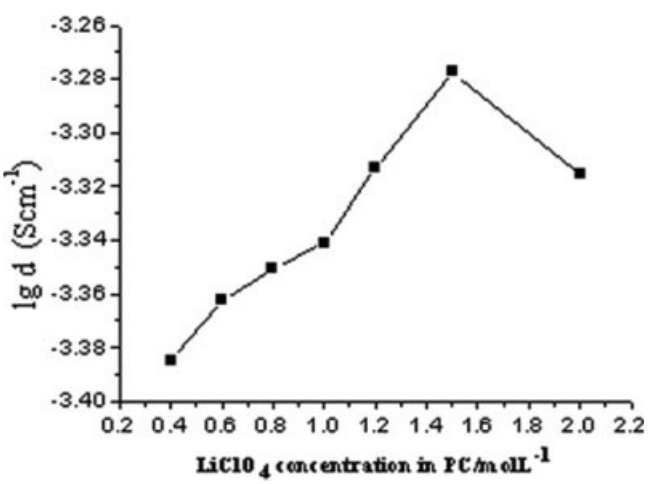

Figure 1 Variation of the room temperature ionic conductivity of gel polymeric electrolyte as a function of $LiClO_4$ concentration in PC at 25°C.

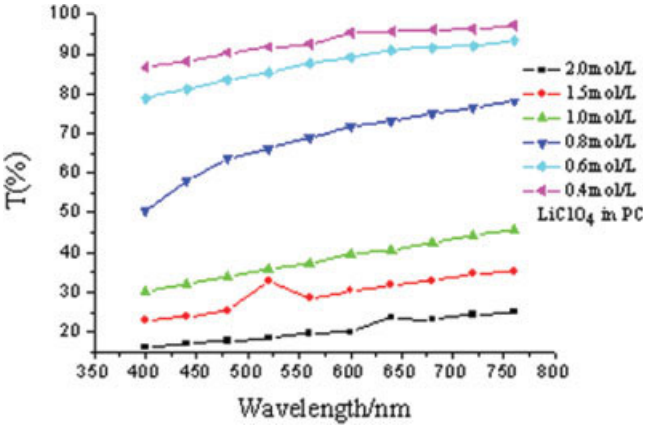

Figure 2 Variation of transmittivity of the GPE membranes as a function of $LiClO_4$ concentration in PC at 25°C in the visible region. [Color figure can be viewed in the online issue, which is available at www.interscience.wiley.com.]

of thin glasses. Transmittance spectra of CPEs were measured using S22 PC model spectrophotometer in a frequency range from 800 to 300 nm (Shanghai, China). The thermal stability of the CPE was investigated using thermogravimetric and differential thermal analysis (TG-DTA) apparatus (model STA 1500, PL Thermal Sciences, UK) in an N_2 flow. The heating rate was 10°C min^{-1}. The surface structure of the CPE was examined by means of scanning electron microscopy (SEM; Hitachi, S-3500 Japan).

RESULTS AND DISCUSSION

Salt concentration effect on gel polymeric electrolyte

Ionic conductivity

Figure 1 shows the variation of conductivity of GPE prepared in step 1 versus $LiClO_4$ concentration in PC at room temperature. The conductivity increases with an increase in salt concentration, reaches a maximum, and decrease at higher concentrations. The highest conductivity value is achieved by a 1.5*M* $LiClO_4$ solution. The following gives an explanation. The more the free ions exist in the CPEs, the higher the ionic conductivity. While ion pairs and ionic aggregations are easily grown with increased salt concentration, which will restrain the mobility of the ions and embarrass the increase of ionic conductivity.[29,30] So, there exists a maximum in conductivity at salt concentration.

Transmittivity

Figure 2 reveals that the transmittivity of the GPE membrane decreases with increasing lithium salt concentrations in electrolytes in the visible region. The highest transmittivity value is achieved by the 0.4*M* $LiClO_4$ solution. The phenomenon is possibly due to the result of either a chemical or the physical cross-linking process between salt and polymer chains, which embarrass the transmission of the light. Some stronger interactions may be established between the salt and polymer chains for higher concentration.

Thus, there is a couple of paradox between conductivity and transmittivity. To attain a good compromise between desirable properties of high room temperature ionic conductivity and transmittance in the visible region, the GPEs containing 0.4 and 1.5*M* $LiClO_4$-PC were mixed with different nanofillers.

Nanofillers' effect on composite polymeric electrolytes

Conductivity

Figure 3 illustrates variation of conductivity values as a function of nanofillers' concentration. As can be seen, conductivity demonstrates a general trend of increase, though by small amount with respect to the GPE. The effect induced by inert fillers is attributed to an increase in the volume fraction of the amorphous phase, which is a prerequisite for higher conductivity. The most noticeable feature is the maximum in conductivity at an optimum weight (0.8 g) of added nanofillers. The addition of the fillers, such as SiO_2 or TiO_2 nanoparticles, decrease polymeric crystallinity[30,31] and result in the enhancement of physical strength as well as the increase in the absorption level of electrolyte solution.[32–34] On the contrary, excessive nanoparticles filling in polymer matrix lead to the aggregation of nanoparticles and decrease the number of the tunnels for lithium ions to migrate in, impede ions movement. So, there is also a maximum in conductivity at filler concentration.

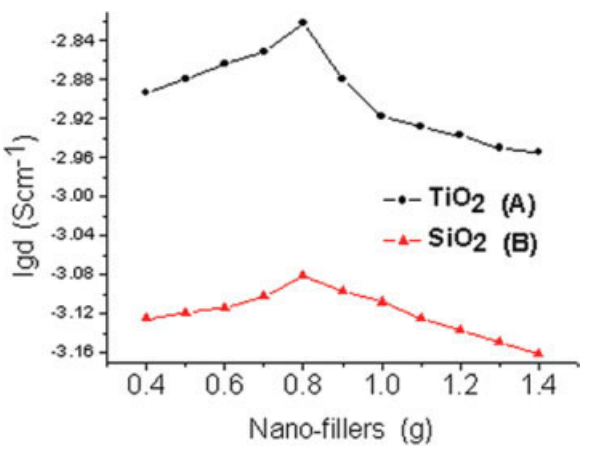

Figure 3 Variation of room temperature ionic conductivity of (A) PMMA (4 g)-Om-POE_n (1 g)-$LiClO_4$ in PC (1.5*M*)-TiO_2 (0.8 g) and (B) PMMA (4 g)-Om-POE_n (1 g)-$LiClO_4$ in PC (0.4*M*)-SiO_2 (0.8 g) as a function of nanofillers content. [Color figure can be viewed in the online issue, which is available at www.interscience.wiley.com.]

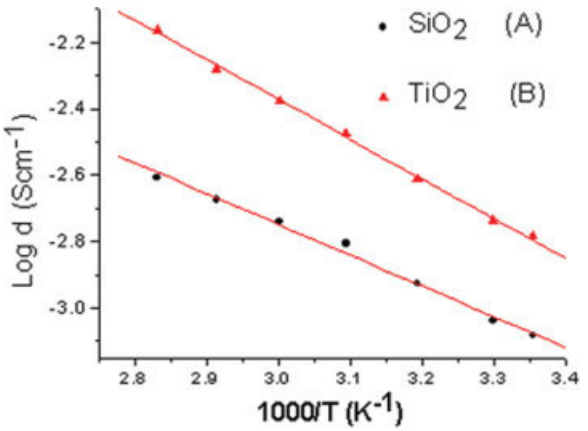

Figure 4 Arrhenius plots of log conductivity against reciprocal temperature for (A) PMMA (4 g)-Om-POE$_n$ (1 g)-$LiClO_4$ in PC (0.4*M*)-gSiO_2(0.8), (B) PMMA (4 g)-Om-POE$_n$ (1 g)-$LiClO_4$ in PC (1.5*M*)-TiO_2 (0.8 g). [Color figure can be viewed in the online issue, which is available at www.interscience.wiley.com.]

Figure 4 shows that the conductivity can be well described by the familiar Arrhenius equation over the temperature range studied. The Arrhenius plots also exemplify an increase in conductivity with temperature. The line fits the equation: $y = -0.9275x + 0.0342$, $R^2 = 0.9926$ for curve A, and the line fits the equation $y = -1.1831x + 1.1762$, $R^2 = 0.9903$ for curve B.

Transmittivity

Figure 5 shows that the transmittivities of CPE membrane vary over the range 74–90% in the visible region, and the highest room temperature conductivity was obtained after the addition of 0.8 g of SiO_2. So, it is a promising electrolyte for an all-solid-state transport electrochromic windows using WO_3 and NiO_x as the electrodes.

While the CPE membranes containing TiO_2 possess the higher conductivities than that containing SiO_2, they can be used only as plate display material because of their opacity.

X-ray diffraction

The X-ray diffraction patterns (Fig. 6) suggested that the systems (A), (D), (E), and (F) are amorphous. The intensity of the crystalline peaks decreases after blending the PMMA and Om-POE$_n$ contrasting between systems (B) and (C) obviously. Continue to add salt solution to system (C), the GPE (D) became amorphous because the crystalline peaks are absent. The intensity of the crystalline peaks also decreases on the addition of fillers. The effect of the filler on the crystallinity of the electrolyte is lower than that caused by lithium salt solution. This indicates that the amount of elastomeric phase (amorphous) increases to some extent as the salt concentration is increased. So, the CPE prepared in this paper is homogenous.

FTIR spectroscopy

FTIR is a powerful tool to study the local structural changes. The FTIR plots of pure PMMA, Om-POE$_n$, and polymer electrolyte complexes are shown in Figure 7. The FTIR spectra of the samples were recorded in the transmittance mode.

The curve F shows the IR spectrum of Om-POE$_n$. The strong infrared absorptions at 2871, 1458, and 1351 cm^{-1} correspond to the CH_2 stretching and bending of the Om-POE$_n$. The absorption bands at 1109, 1038, and 949 cm^{-1} are attributed to the —C—O—C— of the polymer. Because of the strong absorption, it is illuminated that ethylene glycol was linked by ether oxygen bond.

The curve A shows the IR spectrum of PMMA. For pure PMMA contains a carbonyl group, yielding a γ(C=O) stretching mode at 1729 cm^{-1}. Hydrogen bonding of the C=O groups of PMMA would lead to a shift to lower frequencies of this mode.[35] The asymmetry absorption bands at 2995 cm^{-1} and at 2952 $cm^{-1}$are attributed to the CH_3—O and α—CH_3 of the PMMA respectively. The absorption bands seen at 1481 and 1388 cm^{-1} are characteristic of the α—CH_3 asymmetry scissoring and symmetry scissoring respectively. A scissoring band of the CH_3—O group is located at 1448 cm^{-1}. The stretching band at 1151 cm^{-1} is attributed to the C—C. A spectrum of PMMA reveals peaks at 1151, 1068, and 988 cm^{-1} corresponding to the —C—O—C— of the ester group in PMMA.

The bands at 2995 and 2952 cm^{-1} in curve A and the band at 2871 cm^{-1} in the curve F almost combine to produce a single band at 2945 cm^{-1} in the curve B. The frequencies of ester group shows no deviation from its position obviously, but the corresponding

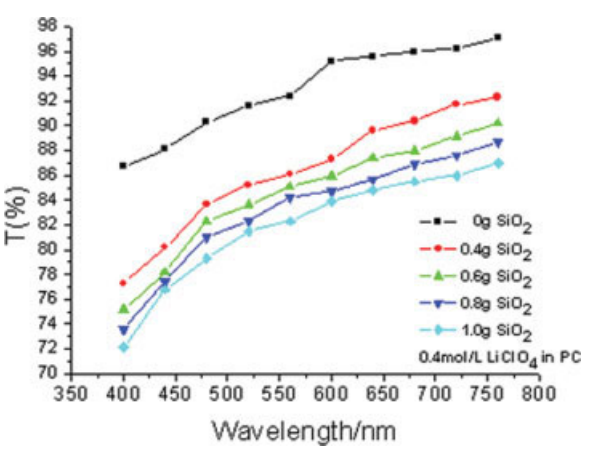

Figure 5 Variation of transmittivity of the CPE membranes as a function of SiO_2 concentration at 25°C in visible region. [Color figure can be viewed in the online issue, which is available at www.interscience.wiley.com.]

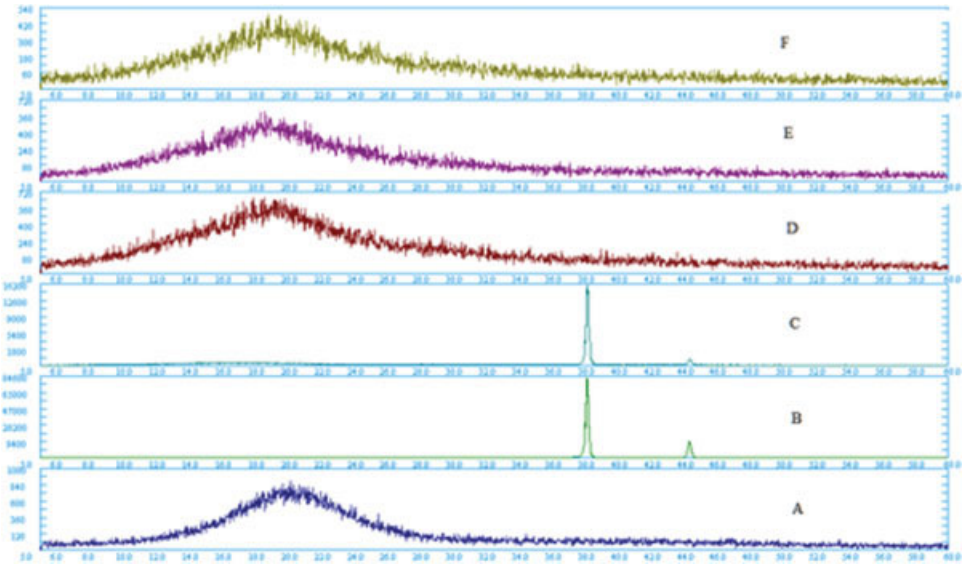

Figure 6 X-ray diffraction spectrum of (A) Om-POE$_n$, (B) PMMA, (C) PMMA (4 g)-Om-POE$_n$ (1 g), (D) PMMA (4 g)-Om-POE$_n$ (1 g)-$LiClO_4$ in PC (1.5*M*), (E) PMMA (4 g)-Om-POE$_n$ (1 g)-$LiClO_4$ in PC (0.4*M*)-SiO_2 (0.8 g), (F) PMMA (4 g)-Om-POE$_n$ (1 g)-$LiClO_4$ in PC (1.5*M*)-TiO_2 (0.8 g). [Color figure can be viewed in the online issue, which is available at www.interscience.wiley.com.]

peak of ester group (1151 cm^{-1}) and the peak (1109 cm^{-1}) assigned to the —C—O—C— of Om-POE$_n$ combine to produce a single broad band (1174 cm^{-1}). The characteristic frequencies of PMMA (949, 1458, and 1448 cm^{-1}) are shifted to (979, 1452, and 1452 cm^{-1}) in the system B. The band of PMMA (988 cm^{-1}) is absent in the system B. The appearances of new peaks along with changes in the exiting peaks in the FTIR spectra confirm the formation of new chemical bonds in the blend polymer, which will help to increase the stability and mechanical character of the system.

After adding the liquid electrolyte solution, the band in curve B at 2945 cm^{-1} splits two components at 2990 and 2953 cm^{-1} in curve C, and the intensity

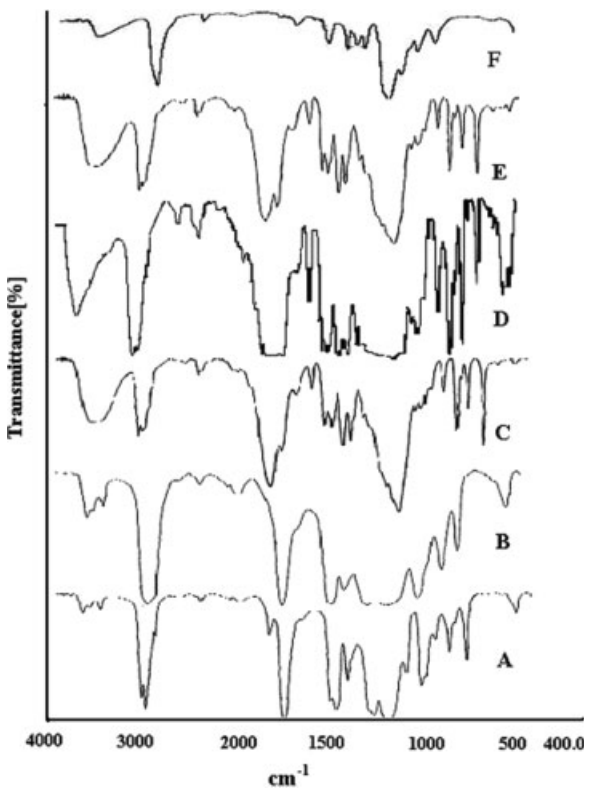

Figure 7 FTIR spectra of (A) PMMA, (B) PMMA (4 g)-Om-POE$_n$ (1 g), (C) PMMA (4 g)-Om-POE$_n$ (1 g)-$LiClO_4$ in PC (1.5*M*), (D) PMMA (4 g)-Om-POE$_n$ (1 g)-$LiClO_4$ in PC (0.4 M)-SiO_2 (0.8 g), (E) PMMA (4 g)-Om-POE$_n$ (1 g)-$LiClO_4$ in PC (1.5*M*)-TiO_2 (0.8 g), (F) Om-POE$_n$.

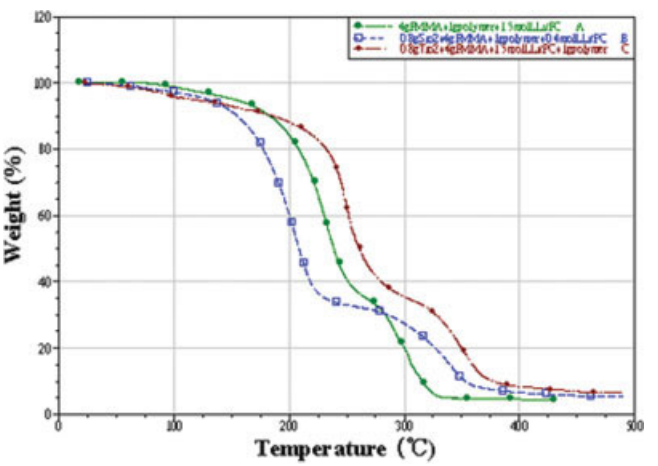

Figure 8 TGA traces of (A) PMMA (4 g)-Om-POE$_n$ (1 g)-$LiClO_4$ in PC (1.5*M*), (B) PMMA (4 g)-Om-POE$_n$ (1 g)-$LiClO_4$ in PC (0.4*M*)-SiO_2 (0.8 g), and (C) PMMA (4 g)-Om-POE$_n$ (1 g)-$LiClO_4$ in PC (1.5*M*)-TiO_2 (0.8 g) at a heating rate of 10°C min^{-1}. [Color figure can be viewed in the online issue, which is available at www.interscience.wiley.com.]

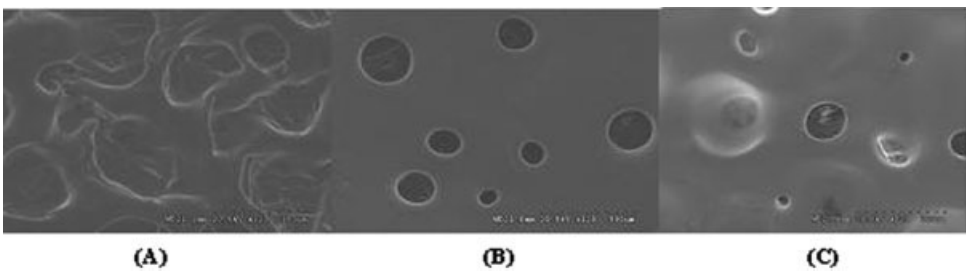

Figure 9 SEM of (A) PMMA (4 g)-Om-POE$_n$ (1 g)-$LiClO_4$ in PC (1.5*M*), (B) PMMA (4 g)-Om-POE$_n$ (1 g)-$LiClO_4$ in PC (0.4*M*)-SiO_2 (0.8 g), and (C) PMMA (4 g)-Om-POE$_n$ (1 g)-$LiClO_4$ in PC (1.5*M*)-TiO_2 (0.8 g) (×120).

decreases. The characteristic frequencies of complexes B (1729, 1174, and 979 cm^{-1}) are shifted to (1731, 1086, and 992 cm^{-1}) in the complexes C respectively. These absorption peaks are shifted by 2, 88, and 13 cm^{-1}. The data show that the alkali metal cations are coordinated to the blend polymer.

Contrast among the complexes C, D, and E, the band at 1086 cm^{-1} in complex C shifts to 1089 cm^{-1} in complex D and 1085 cm^{-1} in the complex E respectively, after addition of the SiO_2 and TiO_2. The shift is due to the interaction between hydroxyl of nanofillers and complex C possibility.

Thermogravimetric analysis

To have an appropriate temperature range of operation, CPEs must have good thermal stability. Figure 8 illustrates thermogravimetric analysis (TGA) traces of three kinds of CPEs synthesized in this paper. The TGA curves indicate no weight loss up to 100°C, but beyond that up to about 350°C, there is continuous weight loss with the same rate.

SEM studies

From the micrographs it is observed that the morphology consisted of a porous structure. Such microporous surface morphology will be helpful to contain the more liquid electrolyte solution and increase the ionic conductivity. A porous structure with small and uniform pores is preferred for lithium battery applications because these pores act as a passage for Li^+ ions during the charge–discharge cycle.[35] What's more, Figure 9 reveals that the three kinds of CPEs are amorphous, which is similar to the results of X-ray studies.

CONCLUSIONS

In this investigation, the transmittivity and room temperature ionic conductivity of every polymer electrolyte membranes in the visible region were studied in detail. The interaction of polymer–salt complex has been confirmed using FTIR spectral studies. The X-ray diffraction patterns suggested that the CPEs prepared in this paper are all amorphous and homogenous. TGA curves revealed that thermal stability of CPEs was up to 100°C.

Furthermore, it is most important that the two CPE systems, which are fit for ECD, were found out, because the ECD need such polymer electrolytes with higher room temperature ionic conductivity, higher optical clarity in the visible region, good mechanical properties, and thermal stability at the same time.

1. The maximum value of conductivity 1.8 mS cm^{-1} is obtained for the PMMA (4 g)-Om-POE$_n$ (1 g)-$LiClO_4$ in PC (0.4*M*, 10 mL)-SiO_2 (0.8 g) CPE film at 298 K with the high optical clarity in the visible region and thermal stability. So, it is a promising electrolyte for all-solid-state transparent ECDs such as ''smart windows''.
2. CPEs prepared by dispersing nanofillers of TiO_2 exhibit high ionic conductivity with good thermal stability and are applied for plate display material because of their opacity.

References

1. Scrosati, B. Application of Electroactive Polymers; Chapman and Hall: London, 1993.
2. Bertier, C.; Gorechi, W.; Mimier, M.; Armand, M. B.; Chabagno, J. M.; Rigaud, P. Solid State Ionics 1983, 11, 91.
3. Cazzanelli, E.; Mariotto, G.; Appetecchi, G. B.; Croce, F.; Scrosati, B. Electrochim Acta 1995, 40, 2379.
4. Ostrovskii, D.; Brodin, A.; Torell, L. M.; Appetecchi, G. B.; Scrosati, B. J Chem Phys 1998, 109, 7618.
5. Ostrovskii, D.; Torell, L. M.; Appetecchi, G. B.; Scrosati, B. Solid State Ionics Diffusion React 1998, 106, 19.
6. Adebahr, J.; Gavelin, P.; Ostrovskii, D.; Torell, L. M.; Wesslen, B. J Mol Struct 1999, 482, 487.
7. Appetecchi, G. B.; Croce, F.; Dautzenberg, G.; Gerace, F.; Panero, S.; Spila, E.; Scrosati, B.; Gazz Chim Ital 1996, 126, 405.
8. Ward, I. M.; Williamson, M. J.; Hubbard, H. V. S. A.; Southall, J. P.; Davies, G. R. J Power Sources 1999, 81, 700.
9. Rajendran, S.; Kannan, R.; Mhendran, O. J Power Sources 2001, 96, 406.
10. Rajendran, S.; Mahendran, O.; Mahalingam, T. Eur Polym J 2002, 38, 49.
11. Myoung, K. P.; Jinhwan, K. Electrochem Commun 2001, 3, 28.
12. Jannasch, P. Polymer 2001, 42, 8629.

13. Ren, T. B.; Huang, X. B.; Zhao, X. A.; Tang, X. Z. J Mater Sci 2003, 28, 3007.
14. Silva, G. G.; Marzana, B. E. J Mater Sci 2000, 35, 4721.
15. Appetecchi, G. B.; Croce, F.; Sciosati, B. Electrochim Acta 1995, 40, 991.
16. Weston, J. E.; Steel, B. C. H. Solid State Ionics 1982, 7, 75.
17. Croce, F.; Mariotto, B. S. Chem Mater 1992, 4, 1134.
18. Hou, J.; Baker, G. L. Chem Mater 1998, 10, 3311.
19. Hou, X. P.; Siow, K. S. Solid State Ionics 2002, 147, 391.
20. Pennarun, P. Y.; Jannasch, P.; Papaefthimiou, S.; Skarpentzos, N.; Yianoulis, P. Thin Solid Films 2006, 514, 258.
21. Chu, P.; Jen, H.; Lo, F.; Lang, C. Macromolecules 1999, 32, 4738.
22. Rajendran, S.; Kannan, R.; Mhendran, O. J Power Sources 2001, 96, 406.
23. Borkowska, R.; Laskowski, J.; Plocharski, J.; Przyluski, J.; Wieczorek, W. J Appl Electrochem 1993, 23, 991.
24. Wieczorek, W.; Florjanczyk, Z.; Stevens, J. R. Electrochim Acta 1995, 40, 2251.
25. Quartarone, E.; Mustarelli, P.; Magistris, A. Solid State Ionics 1998, 110, 1.
26. Kawa, T.; Abe, K.; Honda, K.; Tsuchida, E. J Polym Sci Polym Chem Ed 1975, 13, 1505.
27. Vincent, C. A.; Maccallum, J. R. Polymer Electrolyte Review; Elsevier: London, 1987; p 164.
28. Christian, V.; Nicholas, D. J.; Wilson, C. B. Br Polym J 1988, 20, 289.
29. Torrle, L. M.; Schantz, S. In Polymer Electrolyte Reviews—2; MacCallum, J., Vincent, C. A., Eds.; 1989.
30. Croce, F.; Appetecchi, G. B.; Persi, L.; Scrosati, B. Letters to Nature 1998, 394, 456.
31. Wieczorek, W.; Such, K.; Chung, S. H. J Phys Chem 1994, 98, 9047.
32. Kim, K. M.; Park, N.; Ryu, K. S.; Chang, S. H. Polym J 2002, 43, 3951.
33. Caillon-Caravanier, M.; Claude-Montigny, B.; Lemordant, D.; Bosser, G. J Power Sources 2002, 107, 125.
34. Wang, B.; Gu, L. Mater Lett 2002, 57, 361.
35. Uma, T.; Mahalingam, T.; Stimming, U. Mater Chem Phys 2005, 90, 245.